SIAM J. APPL. MATH.
Vol. 0, No. 0, pp. 000–000
© 200X Society for Industrial and Applied Mathematics

HOPF BIFURCATION IN QUASI-GEOSTROPHIC CHANNEL FLOW*

ZHI-MIN CHEN†, MICHAEL GHIL‡, ERIC SIMONNET§, AND SHOUHONG WANG¶

This paper is dedicated to the memory of Jacques-Louis Lions

Abstract. In this article, we conduct a rigorous stability and bifurcation analysis for a highly idealized model of planetary-scale atmospheric and oceanic flows. The model is governed by the two-dimensional, quasi-geostrophic equation for the conservation of vorticity in an east-west oriented, periodic channel. The main result is the existence of Hopf bifurcation of the flow as the Reynolds number crosses a critical value.

The key idea in proving this result is translating the eigenvalue problem into a difference equation and treating the latter by continued-fraction methods. Numerical results are obtained by using a finite-difference scheme with high spatial resolution and these results agree closely with the theoretical predictions. The spatio-temporal structure of the limit cycle corresponds to a wave that propagates slowly westward and is symmetric about the midaxis of the channel. For plausible paramater values that correspond to midlatitude atmospheric flows, the period of this wave is 20–25 days.

Key words. quasi-geostrophic channel flow, Hopf bifurcation, atmospheric and oceanic waves

AMS subject classifications. 35Q30, 86A05, 86A10, 76E20, 58C40

DOI. 10.1137/S0036139902406164

1. Introduction.

A key problem in the study of climate dynamics is to understand and predict the periodic, quasi-periodic, aperiodic, and fully turbulent characteristics of large-scale atmospheric and oceanic flows. Bifurcation theory enables one to determine how qualitatively different flow regimes appear and disappear as control parameters vary; it provides us, therefore, with an important method to explore the theoretical limits of predicting these flow regimes. In the present paper, we study bifurcations of the original partial differential equations (PDEs) that govern geophysical flows, whereas most studies so far have only considered systems of ordinary differential equations (ODEs) that are obtained by projecting the PDEs onto a finite-dimensional solution space, either by finite differencing or by truncating a Fourier expansion (see Ghil and Childress [10] and further references there). The present approach should allow us to overcome some of the inherent limitations of the numerical bifurcation results that dominate the climate dynamics literature up to this point, and to capture the essential dynamics of the governing PDE systems.

*Received by the editors April 23, 2002; accepted for publication (in revised form) June 20, 2003; published electronically DATE.
http://www.siam.org/journals/siap/x-x/40616.html

†Nankai Institute of Mathematics, Nankai University, Tianjin 300071, People's Republic of China (zhimin@nankai.edu.cn). The research of this author was supported in part by the National Natural Science Foundation of China.

‡Department of Atmospheric Sciences and Institute of Geophysics and Planetary Physics, University of California Los Angeles, Los Angeles, CA 90095-1567 and Département Terre-Atmosphère-Océan, Ecole Normale Supérieure, Paris, France (ghil@atmos.ucla.edu, http://www.atmos.ucla.edu/tcd). The research of this author was supported in part by the National Science Foundation under grant ATM-0082131.

§Institut Nonlinéaire de Nice, UMR 6618 CNRS 1361, route des Lucioles 06560 Valbonne - France (eric.simonnet@inln.cnrs.fr). The research of this author was supported in part by the Department of Energy under grant DE-FG02-01ER63251 to MG.

¶Department of Mathematics, Indiana University, Bloomington, IN 47405 (showang@indiana.edu, http://www.indiana.edu/~fluid). The research of this author was supported in part by the Office of Naval Research under grant N00014-96-1-0425 and by the National Science Foundation under grant DMS-0072612.

The basic equations of large-scale atmospheric and oceanic circulation are the primitive equations. These equations can be derived from the full Navier–Stokes equations *with gravity, rotation, and variable density* by neglecting vertical accelerations (the so-called hydrostatic approximation) and compressibility effects (i.e., sound waves); see Ghil and Childress [10], Kalnay [21], Lions, Temam, and Wang [24, 25], and Pedlosky [36]. One philosophy in the geosciences is to study in great detail simplified models that approximate well the dominant balance of forces on the planetary-scale atmospheric and oceanic flows before addressing the more complete PDE systems that govern these flows in all their complexity. By starting with models that incorporate only the most important effects, and by gradually bringing in others, one is able to proceed inductively and thereby avoid the pitfalls inevitably encountered when a great many poorly understood factors are introduced all at once.

The ideas of dynamical systems theory and nonlinear functional analysis have been applied so far to climate dynamics mainly by careful numerical studies. These were pioneered by Lorenz [26, 27], Stommel [43], and Veronis [44, 45] among others, who explored the bifurcation structure of low-order models of atmospheric and oceanic flows. More recently, pseudoarclength continuation methods have been applied to atmospheric (Legras and Ghil [23]) and oceanic (Speich, Dijkstra, and Ghil [42] and Dijkstra [9]) models with increasing horizontal resolution. These numerical bifurcation studies have so far produced fairly reliable results for two classes of geophysical flows: (i) atmospheric flows in a periodic midlatitude channel, in the presence of bottom topography and a forcing jet; and (ii) oceanic flows in a rectangular midlatitude basin, subject to wind stress on its upper surface. In both cases, the symmetry properties of the forcing have a decisive effect on the bifurcations that arise—saddle-node (Charney and DeVore [6] and Pedlosky [35]) or Hopf (Legras and Ghil [23] and Jin and Ghil [19]) in the atmospheric channel and saddle-node, pitchfork, or Hopf [2, 4, 14, 16, 18, 32, 42] in the oceanic basin.

More recently, the role of global bifurcations, via homoclinic and heteroclinic orbits, has been demonstrated numerically in the wind-driven ocean circulation problem, for both shallow-water (Chang et al. [5], Simonnet et al. [40, 41]) and quasi-geostrophic (QG) (Meacham [31] and Nadiga and Luce [34]) models. Both of these models represent further simplifications of the primitive equations [10, 36]. Still, the only mathematically rigorous proof of a bifurcation in either the atmospheric or the oceanic problem outlined here appears, as far as we know, in the work of Wolansky [47, 48], and it extends solely to the existence of asymmetric stationary solutions.

The present paper addresses the somewhat more difficult problem of proving the existence of Hopf bifurcation in a QG flow in two dimensions. The main difficulty in solving this problem is in estimating the crucial information on the spectrum of the problem linearized around the basic flow. The main objective of this article is to overcome this difficulty and bring a new set of tools to the rigorous study of successive bifurcations in geophysical fluid dynamics problems.

More precisely, we conduct a bifurcation analysis of the following idealized two-dimensional (2-D) QG flow problem. The governing equation dictates the conservation of vorticity, as modified by forcing and dissipation:

$$\partial_t \Delta\psi + \varepsilon J(\psi, \Delta\psi) + \partial_x \psi = E\Delta^2\psi - \tau_0 \sin \pi y, \tag{1.1}$$

where $\psi = \psi(x, y, t)$ is a streamfunction and $J(\psi, \phi) = \partial_x\psi\partial_y\phi - \partial_y\psi\partial_x\phi$ is the advection operator. The x-axis is directed to the east and the y-axis to the north. The zonal and meridional velocity components u and v are obtained from the streamfunction by

$$u = -\psi_y, \qquad v = \psi_x.$$

The relative vorticity ξ and the streamfunction ψ are related by the Poisson equation

$$\Delta\psi = \xi.$$

Equation (1.1) is derived from either the shallow-water equations with rotation or the primitive equations by the so-called QG approximation, which assumes that the balance between the Coriolis force and the pressure gradient dominates the flow. This approximation corresponds to a singular perturbation that filters out the Poincaré waves, also called inertia-gravity waves (i.e., gravity waves modified by the presence of rotation). The QG equation (1.1) only supports Rossby waves, whose phase velocity—in the absence of forcing and dissipation, i.e., with a zero right-hand side—is comparable to the characteristic particle velocity; see Ghil and Childress [10] and Pedlosky [36]. Wolansky [48] studied the so-called barotropic, 2-D version of the QG model (1.1), while Wang [46] obtained results on existence, uniqueness, and long-time dynamics of the so-called baroclinic, three-dimensional (3-D) version.

The flow domain is a rectangular region $\Omega = \{(x, y);\ 0 \leq x \leq 2/a;\ 0 \leq y \leq 2\}$. For simplicity, we use here only the zonal component of the forcing. In an atmospheric model, this forcing represents—in the QG vorticity equation (1.1), in which there are no explicit thermodynamic effects—the transfer of angular momentum into midlatitudes due to the tropical Hadley cell (Lorenz [28]). Alternatively, one can think about a zonal forcing jet that would be in perfect geostrophic equilibrium with the pole-to-equator temperature gradient (Lorenz [27] and Ghil and Childress [10]).

In an oceanic model, the time-and-longitude independent forcing on the right-hand side of (1.1) is the curl of the wind stress

$$\nabla \times \tau = -\tau_0 \sin \pi y;$$

a wind stress of the form $\tau = -\tau_0(\cos \pi y, 0)$ mimics the annually averaged zonal wind distribution over the North Atlantic or North Pacific, with westerly (i.e., eastward) winds over the midlatitudes and easterlies in the tropics and polar latitudes.

The parameters ε and E are positive constants, called the Rossby and Ekman numbers, respectively. They measure the relative importance of nonlinearity and lateral diffusion. The effect of the bottom friction is neglected in this article. The Reynolds number is defined here as

$$R = \frac{\varepsilon}{E}.$$

The unknown streamfunction ψ satisfies periodic boundary conditions at $x = 0, 2/a$ and free-slip boundary conditions at $y = 0, 2$:

$$\begin{cases} \psi(t, 2/a, y) = \psi(t, 0, y), \\ \psi(t, x, 0) = \psi(t, x, 2) = 0;\ \partial_y^2\psi(t, x, 0) = \partial_y^2\psi(t, x, 2) = 0. \end{cases} \tag{1.2}$$

Along the meridional boundaries $y = 0, 2$, $\Delta\psi = \partial_y^2\psi = -\partial_y u$, and $u_y = 0$ corresponds to free slip along these boundaries. More general, "partial-slip" boundary conditions—intermediate between free slip and no slip ($u = -\psi_y = 0$)—are discussed in Appendix A of [18] for the 2-D shallow-water equations and in [14] for a 3-D version of the QG equations.

It is readily seen that (1.1) with (1.2) admits the steady-state solution $\psi_0 = \psi_0(y)$, where

$$\psi_0 = \frac{\tau_0}{\pi^4 E} \sin \pi y. \tag{1.3}$$

We shall take $\tau_0 = 1$ below for simplicity.

This midlatitude channel with zonal periodicity is a better model for the atmospheric problem that we outlined above than for the oceanic one. Still, the methods we apply might eventually be extended to the latter. As mentioned already, Wolansky [47] studied existence, uniqueness, and stability of stationary solutions of (1.1) in the presence of topography and free-surface effects, which are omitted here. Wolansky [48] showed, for a domain bounded by a closed streamline and nondivergent forcing, that sufficient conditions exist under which a branch of asymmetric stationary solutions bifurcates from the symmetric branch obtained when the domain, as well as the forcing, admits a symmetry group. His results were shown to apply in an infinite channel with the symmetry group of zonal translations.

The main objective of this article is to prove the following theorem.

THEOREM 1.1.

(i) *Let $a \geq \sqrt{3}/2$ and $E > 0$. Then* (1.1) *and* (1.2) *are linearly stable around ψ_0 for any Reynolds number $R > 0$, where $\psi_0 = \psi_0(y)$ is given by* (1.3).

(ii) *Let $\sqrt{3}/4 \leq a \leq \alpha_0$ and $E > 0$. Then there exists a critical Reynolds number $R_0 > 0$ for* (1.1) *and* (1.2). *Moreover* (1.1) *and* (1.2) *admit a nontrivial, time-periodic, classical solution ψ_R branching off ψ_0 as the Reynolds number R crosses R_0, provided that $E > c_0$ for some constant $c_0 > 0$.*

This theorem is based essentially on the eigenvalue analysis of the spectral problem with respect to the linearization of (1.1) and (1.2) around ψ_0, by using the continued-fraction method first introduced by Meshalkin and Sinai [33]. For the 2-D Navier–Stokes equations, without the Coriolis term and with periodic boundary conditions in both the x and y directions, stability and bifurcation were studied in [7, 17, 33]. For the 3-D Navier–Stokes equations, without the Coriolis term and with periodic boundary conditions in three directions, pitchfork bifurcation was studied by Chen and Wang [8]. They showed that the bifurcated branches exist for all Reynolds number values past the critical one and that the stationary solutions on these branches stay bounded as $R \to \infty$.

For 2-D incompressible viscous flows with periodic boundary conditions, Meshalkin and Sinai [33] deduced the linear stability of the steady state (1.3) when $a = 1$ with respect to all Reynolds numbers, Iudovich [17] proved the existence of steady-state bifurcation when $0 < a < 1$, and Chen and Price [7] obtained the existence of Hopf bifurcation for some a with $0 < a < \sqrt{3}/2$. Steady-state bifurcation, however, no longer occurs for any a under the free-slip boundary conditions described by (1.2).

In the present paper, the constant a is bounded from below by $\sqrt{3}/4$ for Hopf bifurcation to occur. In fact, for $0 < a < \sqrt{3}/4$ multiple pairs of eigenvalues crossing the imaginary line do occur, and by applying our approach here in a more sophisticated manner, the existence of time-periodic solutions can also be proven rigorously in this case; this will be reported elsewhere. Numerically, the multiple periodic solutions are found in section 6 here (Figures 6.2 and 6.3).

To prove assertion (ii) of Theorem 1.1 requires verifying a transversal crossing condition; see (1.7) below. This verification is rendered more difficult by the presence of the so-called β-term $\partial_x \psi$ in (1.1), which arises due to the meridional gradient of the planetary vorticity [10, 36]. In order to prove the validity of this condition, we have to assume that $E > c_0$ for some constant c_0, although numerical experiments reveal the occurrence of Hopf bifurcation for large τ_0 but small E [14, 18, 40, 41, 42]. Technical difficulties prevent us from covering in Theorem 1.1 the range of x-periods given by $\alpha_0 < a < \sqrt{3}/2$, with $3/4 < \alpha_0 \simeq 0.8$. The overall situation for our QG channel flow, governed by (1.1), (1.2), is illustrated in Figure 1.1.

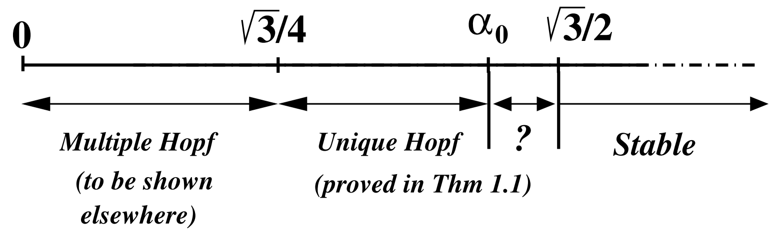

FIG. 1.1. *Range of values of the channel aspect ratio a for which various assertions hold. The equivalence between the spectral problem* (1.5) *with boundary conditions* (1.2) *and the difference equation of* (2.5)–(2.10) *holds for* $\sqrt{3}/4 \le a \le \sqrt{3}/2$ *(see Lemma* 2.2 *below). The numerical results in Figure* 6.2 *indicate that Hopf bifurcation also occurs for* $\alpha_0 \le a < \sqrt{3}/2$.

To prove Theorem 1.1, we decompose the streamfunction into a stationary part $\psi_0(x, y)$ given by (1.3) and a perturbation with exponential time dependence

$$\psi(x, y, t) = e^{\rho t}\phi(x, y), \tag{1.4}$$

where ϕ satisfies the boundary conditions (1.2). Introducing this solution into the governing equation and linearizing the latter with respect to the amplitude of the perturbation, we obtain the spectral problem

$$\rho\Delta\phi + \varepsilon\left(\partial_x\phi\,\partial_y\Delta\psi_0 - \partial_y\psi_0\,\partial_x\Delta\phi\right) + \partial_x\phi = E\Delta^2\phi.$$

Substituting the basic solution ψ_0 from (1.3) yields

$$L(\rho)\phi \doteq \left(E\Delta^2 - \partial_x + \frac{R}{\pi^3}\cos\pi y(\pi^2 + \Delta)\partial_x - \rho\Delta\right)\phi = 0. \tag{1.5}$$

The stability assertion (i) in the main theorem, i.e., the nonexistence of an eigenvalue ρ with $\operatorname{Re}\rho \ge 0$ for all $R > 0$, will be obtained by using the argument that Meshalkin and Sinai [33] first applied to the linear stability analysis of the 2-D Navier–Stokes equations.

The main effort is devoted to the proof of the bifurcation assertion (ii) of Theorem 1.1. Using the functional analysis framework of the Hopf bifurcation theorem in an infinite-dimensional setting (Joseph and Sattinger [20], Marsden and McCracken [30]), assertion (ii) of this theorem will follow if the following assertions can be shown to hold:

(a) There exists a critical Reynolds number $R_0 > 0$ and an eigenvalue $\rho = \rho(R_0)$ of (1.2) and (1.5) such that $\operatorname{Re}\rho(R_0) = 0$ and $\operatorname{Im}\rho(R_0) \ne 0$;

(b) this eigenvalue is simple, i.e.,

$$1 = \dim \bigcup_{n\ge 1}\left\{\phi \in H^4; L^n(\rho)\phi = 0\right\}; \tag{1.6}$$

(c) the transversal crossing condition

$$\text{Re}\, \frac{d\rho(R_0)}{dR} > 0. \tag{1.7}$$

Here H^4 denotes the complex space

$$H^4 = \{\phi \in L_2(\Omega);\ \Delta^2\phi \in L_2(\Omega),\ \phi \text{ satisfies } (1.2)\},$$

which contains the solution space of (1.1) and (1.2). This is a Hilbert space in the norm

$$\|\phi\|_{H^4} = \|\Delta^2\phi\|_{L_2(\Omega)}.$$

It is readily seen from the definition of H^4 that the bifurcating solution can be represented in the form of the Fourier expansion

$$\begin{aligned} &\psi(x, y, t) \\ &= \sum_{m=-\infty}^{\infty} \sum_{n\geq 1-k} \sum_{k=0}^{1} (X_{m,n,k}(t) \cos m\alpha\pi x + Y_{m,n,k}(t) \sin m\alpha\pi x) \sin(n + k/2)\pi y. \end{aligned} \tag{1.8}$$

This paper is organized as follows. The rigorous stability and bifurcation analysis of the problem is carried out in sections 2–5. Section 2 contains the proof of assertion (i) and a basic lemma on formulating the spectral problem. The proof of assertion (ii) is completed by combining section 3 on the existence of R_0 and $\rho(R_0)$, section 4 on the simplicity of the eigenvalue $\rho = \rho(R_0)$, and section 5 on the transversal crossing condition (1.7).

These analytical results are verified and complemented by numerical results in section 6. This section also contains comments on the geophysical significance of the periodic solutions. Brief remarks on the role of symmetry breaking in the bifurcation of time-periodic vs. stationary solutions follow in section 7.

2. Stability and equivalent formulation of the spectral problem. To prove the linear stability result of Theorem 1.1 and to obtain an equivalent formulation of the spectral problem, we follow the argument of Meshalkin and Sinai [33] by transforming the spectral problem into a difference equation, which is solved by continued-fraction methods.

As stated already in section 1, the free-slip boundary condition in (1.2) is equivalent to the condition $\phi = \Delta\phi = 0$ at $y = 0$ and $y = 2$. An application of this condition to (1.5) yields the generalized boundary condition

$$\Delta^n\phi = 0, \text{ at } y = 0 \text{ and } y = 2 \quad (n = 0, 1, 2, \ldots).$$

Thus the general expansion of the unknown function $\phi \in H^4$ for the spectral problem represented by (1.2) and (1.5) takes the form

$$\phi(x, y) = \sum_{m=-\infty}^{\infty} \sum_{n\geq 1-k} \sum_{k=0}^{1} e^{im\alpha\pi x} i^n \phi_{n,m,k} \sin(n + k/2)\pi y, \quad i = \sqrt{-1}\ . \tag{2.1}$$

The fact that i^n appears explicitly in the coefficients of this expansion is only for convenience of notation in the derivation.

Note that no bifurcation can occur for Reynolds number R for which the corresponding eigenvalue ρ lies in the complex half-plane $\text{Re}\rho < 0$. In order to obtain our stated bifurcation result, it is necessary to specify all of the eigenvalues ρ with $\text{Re}\rho \geq 0$ and their corresponding eigenfunctions. However, the general expression of the eigenfunction in (2.1) is too complicated for this purpose. Fortunately, the eigenfunctions can be expressed in a simpler form, as given by the following lemma.

LEMMA 2.1. *Let $a \geq \sqrt{3}/4$ and let ρ be an eigenvalue of* (1.2) *and* (1.5) *such that $\text{Re}\rho > -E\pi^2(a^2+1/4)$. Then $a < \sqrt{3}/2$ and the corresponding eigenfunction has the form*

$$\phi(x,y) = e^{\pm ia\pi x}\sum_{n=0}^{\infty} i^n \phi_n \sin(n+1/2)\pi y. \tag{2.2}$$

Proof. To begin with, we show that for given integers m and $k=0,1$, the subspace of H^4

$$\left\{\phi \in H^4;\ \phi = \sum_{n\geq 1-k} e^{ima\pi x} i^n \phi_n \sin(n+k/2)\pi y\right\} \tag{2.3}$$

is invariant with respect to the spectral operator $\Delta^{-2}L(\rho)$, L being defined by (1.5).

For ϕ in the previous subspace, we see that

$$\begin{aligned}
&e^{-ima\pi x}L\phi \\
&= \sum_{n\geq 1-k}\{\pi^2[m^2a^2+(n+k/2)^2]\rho - ima\pi\} i^n\phi_n \sin(n+k/2)\pi y \\
&\quad + \sum_{n\geq 1-k} E\pi^4[m^2a^2+(n+k/2)^2]^2 i^n \phi_n \sin(n+k/2)\pi y \\
&\quad - R\sum_{n\geq 1-k} a[a^2+(n+k/2)^2-1] i^{n+1}\phi_n \cos\pi y \sin(n+k/2)\pi y \\
&= \sum_{n\geq 1-k}\{\pi^2[m^2a^2+(n+k/2)^2]\rho - ima\pi\} i^n\phi_n \sin(n+k/2)\pi y \\
&\quad + \sum_{n\geq 1-k} E\pi^4[m^2a^2+(n+k/2)^2]^2 i^n \phi_n \sin(n+k/2)\pi y \\
&\quad - \frac{R}{2}\sum_{n\geq 2-k} ma[m^2a^2+(n-1+k/2)^2-1] i^n \phi_{n-1}\sin(n+k/2)\pi y \\
&\quad + \frac{R}{2}\sum_{n\geq 0} ma[m^2a^2+(n+1+k/2)^2-1] i^n \phi_{n+1}\sin(n+k/2)\pi y \\
&\quad + \frac{R}{2} ma(m^2a^2-3/4) i\phi_0 \sin(k/2)\pi y.
\end{aligned}$$

We thus have

$$L\sum_{n\geq 1-k} e^{ima\pi x} i^n \phi_n \sin(n+k/2)\pi y = \sum_{n\geq 1-k} e^{ima\pi x} i^n \psi_n \sin(n+k/2)\pi y, \tag{2.4}$$

where ψ_n is a linear combination of ϕ_{n-1}, ϕ_n, and ϕ_{n+1}. More precisely, for $n > 1-k$,

$$\begin{aligned}
\psi_n &= \{\pi^2[m^2a^2+(n+k/2)^2]\rho - ima\pi + E\pi^4[m^2a^2+(n+k/2)^2]^2\}\phi_n \\
&\quad - \frac{R}{2}ma[m^2a^2+(n-1+k/2)^2-1]\phi_{n-1} + \frac{R}{2}ma[m^2a^2+(n+1+k/2)^2-1]\phi_{n+1},
\end{aligned}$$

while

$$\begin{aligned}\psi_{1-k} = &\{\pi^2[m^2a^2+(1-k/2)^2]\rho - ima\pi + E\pi^4[m^2a^2+(1-k/2)^2]^2\}\phi_{1-k}\\ &+\frac{R}{2}kma[m^2a^2+(1+k/2)^2-1]\phi_1+\frac{R}{2}kma(m^2a^2-3/4)i\phi_0\\ &+\frac{R}{2}(1-k)ma(m^2a^2+3)\phi_2.\end{aligned}$$

This gives the invariance of the subspace (2.3), and thus we may assume that any eigenfunction ϕ is in this subspace for some integer m and some $k = 0, 1$.

We can now prove the desired assertion. Indeed, suppose that (ρ, ϕ) solves the spectral problem $L(\rho)\phi = 0$ and thus, by (2.4),

$$\psi_n = 0, \;\; n \geq 1-k. \tag{2.5}$$

If $m = 0$, this implies immediately $\phi_n = 0$ for $n \geq 1-k$. If $m \neq 0$, the spectral problem yields

$$\sum_{n\geq 1-k}[m^2a^2+(n+k/2)^2-1]\psi_n\bar{\phi}_n = 0,$$

where $\bar{\phi}_n$ is the complex conjugate of ϕ_n, and so its real part satisfies

$$\sum_{n\geq 1-k}[m^2a^2+(n+k/2)^2]\{\text{Re}\rho+E\pi^2[m^2a^2+(n+k/2)^2]\}[m^2a^2+(n+k/2)^2-1]|\phi_n|^2 = 0. \tag{2.6}$$

This result, together with the condition $\text{Re}\rho + E\pi^2(a^2+1/4) > 0$ and (2.5), implies

$$\begin{cases}\phi_n\equiv 0 & \text{when } k=0, a>0, -\infty<m<\infty,\\ \phi_n\equiv 0 & \text{when } k=1, a>\sqrt{3}/2, -\infty<m<\infty,\\ \phi_n\equiv 0 & \text{when } k=1, \sqrt{3}/4\leq a\leq\sqrt{3}/2, |m|\geq 2,\end{cases}$$

since $m^2a^2 + (n+k/2)^2 - 1 \geq 0$.

The proof is thus complete. □

This lemma immediately gives the stability result contained in assertion (i) of Theorem 1.1.

As we shall see, it is important to realize that $k = 0$ corresponds to a function $\phi(x, y)$ that is antisymmetric about the axis $y = 1$ of the channel, while $\phi(x, y)$ is symmetric about this axis for $k = 1$. It follows from Lemma 2.1 that no bifurcation can arise in the problem governed by (1.1) and (1.2) from an antisymmetric instability.

To address the bifurcation problem, we thus consider the spectral equation (1.5)

$$\rho > -E\pi^2(a^2+1/4), \;\; \phi = \sum_{n=0}^{\infty} e^{\pm ia\pi x} i^n \phi_n \sin(n+1/2)\pi y \in H^4$$

in the case $\sqrt{3}/4 \leq a < \sqrt{3}/2$. For simplicity, let

$$d_n = \frac{2\pi^2[a^2+(n+1/2)^2]\rho - 2a\pi i + 2E\pi^4[a^2+(n+1/2)^2]^2}{Ra[a^2+(n+1/2)^2-1]}; \tag{2.7}$$

it follows, in particular, that Re $d_0 < 0$ and Re $d_n > 0$ with $n \geq 1$.

For the eigenfunction

$$\phi = \sum_{n=0}^{\infty} e^{ia\pi x} i^n \phi_n \sin(n+1/2)\pi y \in H^4, \tag{2.8}$$

let

$$\xi_n = a[a^2 + (n+k/2)^2 - 1]\phi_n. \tag{2.9}$$

The spectral problem $L(\rho)\phi = 0$ is, by (2.4), equivalent to $\psi_n = 0$; see (2.5). With definitions (2.7) and (2.9), the latter formulation becomes

$$\begin{cases} d_0\xi_0 + i\xi_0 + \xi_1 = 0, & n = 0, \\ d_n\xi_n - \xi_{n-1} + \xi_{n+1} = 0, & n \geq 1, \end{cases} \tag{2.10}$$

and (2.6) can be rewritten as

$$\sum_{n\geq 0} \operatorname{Re} d_n |\xi_n|^2 = 0. \tag{2.11}$$

It is readily seen that (2.10) implies that $\xi_n = 0$ for all $n \geq 0$ whenever there exists an $n_0 \geq 0$ for which $\xi_{n_0} = 0$.

Thus we may assume that $\xi_n \neq 0$ for $n \geq 0$. Hence, we obtain from (2.10) that

$$\frac{\xi_1}{\xi_0} = -d_0 - i, \quad \frac{\xi_n}{\xi_{n-1}} = \frac{1}{d_n + \dfrac{\xi_{n+1}}{\xi_n}}, \quad n \geq 1.$$

It follows therewith from (2.8) that $\rho = \rho(R)$ solves the following continued-fraction equation:

$$-d_0 - i = \cfrac{1}{d_1 + \cfrac{1}{d_2 + \cfrac{1}{\ddots}}}. \tag{2.12}$$

Moreover, we see that the spectral problem $L(\rho)\phi = 0$ is equivalent to the complex conjugate spectral problem $L(\bar{\rho})\bar{\phi} = 0$, with

$$\bar{\phi} = \sum_{n=0}^{\infty} e^{-ia\pi x} i^n (-1)^n \bar{\phi}_n \sin(n+1/2)\pi y \in H^4,$$

and thus $(\bar{\rho}, \bar{\phi})$ satisfies the complex conjugate of the three-term recursions (2.10), namely,

$$\begin{cases} \bar{d}_0\bar{\xi}_0 - i\bar{\xi}_0 + \bar{\xi}_1 = 0, & n = 0, \\ \bar{d}_n\bar{\xi}_n - \bar{\xi}_{n-1} + \bar{\xi}_{n+1} = 0, & n \geq 1. \end{cases} \tag{2.13}$$

Note that (2.10) and (2.13) are two distinct difference equations.

The above argument implies the following fundamental lemma.

LEMMA 2.2. *For $\sqrt{3}/4 \le a < \sqrt{3}/2$, the spectral problem described by* (1.5) *and* (1.2) *with unknown spectral solution* (ρ, ϕ) *such that*

$$\mathrm{Re}\rho > -E\pi^2(a^2+1/4), \quad \phi(x,y) = \sum_{n=0}^{\infty} e^{ia\pi x} i^n \phi_n \sin(n+1/2)\pi y \in H^4$$

is equivalent to the difference equation (2.10) *with* (d_n, ξ_n) *satisfying the constraints* (2.7), (2.9), (2.11), *and* (2.12). *Moreover, for a nontrivial eigenfunction ϕ, the corresponding sequence $\{\xi_n\}$ may be represented in the product form*

$$\xi_n = c\gamma_1 \cdots \gamma_n, \quad n \ge 1,$$
$$\xi_0 = c,$$

where c is an arbitrary complex constant and the factors γ_n are given by the infinite continued fractions

$$\gamma_n = \cfrac{1}{d_n + \cfrac{1}{d_{n+1} + \cfrac{1}{\ddots}}}.$$

Furthermore, the spectral problem described by (1.5) *and* (1.2) *with another unknown solution* $(\bar{\rho}, \bar{\phi})$, *the complex conjugate of* (ρ, ϕ), *is equivalent to the difference equation* (2.13).

3. Existence of a critical Reynolds number. In this section, we show the existence of a critical Reynolds number R_0 and the existence of an eigenvalue $\rho(R)$ such that $\mathrm{Re}\,\rho(R_0) = 0$ and $\mathrm{Im}\,\rho(R_0) > 0$. We begin with the existence of the eigenvalue ρ, which may reach, and eventually cross, the imaginary axis of the complex plane.

LEMMA 3.1. *The spectral problem expressed by* (1.5) *and* (1.2) *admits a unique pair of complex conjugate eigenvalues $\rho = \rho(R)$ and $\bar{\rho} = \bar{\rho}(R)$ for any $R > 0$ and $\sqrt{3}/4 \le a \le \alpha_0$, such that* $\mathrm{Re}\,\rho > -E\pi^2(a^2+1/4)$.

Proof. From Lemma 2.2, we see readily that it suffices to show the existence and uniqueness of a function $\rho = \rho(R)$ that satisfies (2.7)–(2.12). Combining (2.7) and (2.12), we may write $\rho(R)$ as

$$\rho = -E\pi^2(a^2+1/4) + \frac{i2a\pi + iRa(3/4-a^2)}{2\pi^2(a^2+1/4)} + \cfrac{\cfrac{Ra(3/4-a^2)}{2\pi^2(a^2+1/4)}}{d_1 + \cfrac{1}{d_2 + \cfrac{1}{\ddots}}}. \tag{3.1}$$

To derive the existence of the unique pair of eigenvalues that satisfies the required strong inequality, we denote by $\Phi_R(\rho)$ the right-hand side of (3.1). It suffices then to show the existence of a fixed point of Φ_R in the complex plane $\mathbb{C}$. Indeed, since $\mathrm{Re}\rho \ge -E\pi^2(a^2+1/4)$, $R > 0$, and $a^2 < 3/4$, we have

$$\mathrm{Re}\Phi_R(\rho) > -E\pi^2(a^2+1/4)$$

and

$$|\Phi_R(\rho)| \le E\pi^2(a^2+1/4) + \frac{2a\pi + Ra(3/4-a^2)}{2\pi^2(a^2+1/4)} + \frac{Ra(3/4-a^2)}{2\pi^2(a^2+1/4)}\frac{1}{\operatorname{Re} d_1}$$
$$\le E\pi^2(a^2+1/4) + \frac{2a\pi + Ra(3/4-a^2)}{2\pi^2(a^2+1/4)} + \frac{R^2a^2(3/4-a^2)(a^2+5/4)}{8\pi^4(a^2+1/4)(a^2+9/4)E}. \tag{3.2}$$

Denoting this bound by K_R, we see that Φ_R maps the closed convex set

$$C_R = \{z \in \mathbb{C}; -E\pi^2(a^2+1/4) \le \mathrm{Re} z,\ \ |z| \le K_R\} \tag{3.3}$$

into itself. It follows from Brouwer's fixed point theorem that there exists a value $\rho(R)$ in this compact set such that $\Phi_R(\rho(R)) = \rho(R)$. This gives the existence of the desired pair of eigenvalues.

By Lemmas 2.1 and 2.2, we see that there is a one-to-one correspondence between each pair of complex conjugate eigenvalues of the spectral problem $L(\rho)\phi = 0$ and a solution ρ to the difference equation (2.10). In order to show that the pair of eigenvalues is unique, we suppose the existence of two pairs of complex conjugate solutions $\rho_j = \rho_j(R)$ and $\bar\rho_j = \bar\rho_j(R)$, with $\mathrm{Re}\rho_j > -E\pi^2(a^2+1/4)$ for $j = 1, 2$ and $R > 0$. This is equivalent to (2.10) admitting two solutions ρ_j for $j = 1, 2$ such that

$$\gamma_n(\rho_j) = \frac{1}{d_n + \gamma_{n+1}(\rho_j)} = \lim_{m\to\infty} \cfrac{1}{d_n + \cfrac{1}{d_{n+1} + \cfrac{1}{\ddots\, \cfrac{1}{d_{n+m}}}}}$$

for $d_n = d_n(\rho_j)$ defined by (2.7) and $\mathrm{Re}\rho_j > -E\pi^2(a^2+1/4)$. We have

$$\gamma_n(\rho_1) - \gamma_n(\rho_2) = -\gamma_n(\rho_1)\gamma_n(\rho_2)[d_n(\rho_1) - d_n(\rho_2) + \gamma_{n+1}(\rho_1) - \gamma_{n+1}(\rho_2)],$$

and so, by induction,

$$\gamma_1(\rho_1) - \gamma_1(\rho_2) = \sum_{n\ge 1}(-1)^n[d_n(\rho_1) - d_n(\rho_2)]\eta_n(\rho_1)\eta_n(\rho_2)$$
$$= \sum_{n\ge 1}(-1)^n \frac{2\pi[a^2+(n+1/2)^2]}{Ra[a^2+(n+1/2)^2-1]}\eta_n(\rho_1)\eta_n(\rho_2)(\rho_1-\rho_2); \tag{3.4}$$

here $\{\eta_n(\rho_j)\}$ is now the solution specified by Lemma 2.2 such that $\eta_n = \xi_n$ and $\eta_0 = c = 1$. This yields, for $\rho_1 \ne \rho_2$,

$$\begin{aligned}
&|\rho_1 - \rho_2| \\
&= \frac{Ra(3/4-a^2)}{2\pi^2(a^2+1/4)}|\gamma_1(\rho_1) - \gamma_1(\rho_2)| \\
&\le \frac{3/4-a^2}{2(a^2+1/4)}\sum_{n\ge 1}\frac{a^2+(n+1/2)^2}{[a^2+(n+1/2)^2-1]}(|\eta_n(\rho_1)|^2 + |\eta_n(\rho_2)|^2)|\rho_1-\rho_2| \\
&< \frac{3/4-a^2}{2a^2+1/2}\sum_{i=1}^{2}\sum_{n\ge 1}\frac{[a^2+(n+1/2)^2]\{\mathrm{Re}\rho_i + E\pi^2[a^2+(n+1/2)^2]\}}{[\mathrm{Re}\rho_i + E\pi^2(a^2+1/4)][a^2+(n+1/2)^2-1]}|\eta_n(\rho_i)|^2|\rho_1-\rho_2| \\
&= |\rho_1 - \rho_2|,
\end{aligned}$$

where we have used (2.11). The strong inequality implies $\rho_1 = \rho_2$, which completes the proof of Lemma 3.1. ◻

LEMMA 3.2. *Let $\rho = \rho(R)$ with $R > 0$ be one of the two complex conjugate eigenvalues obtained in Lemma* 3.1. *Then we have* $\mathrm{Im}\rho(R) \neq 0$.

Proof. Assuming otherwise, i.e., $\mathrm{Im}\,\rho = 0$, we derive a contradiction. To this end, notice that

$$\begin{aligned}\left|\frac{\mathrm{Im}\,d_n}{\mathrm{Re}\,d_n}\right| &= \frac{\left|(a^2+(n+1/2)^2)\mathrm{Im}\,\rho\pi^2 - a\pi\right|}{\pi^2(a^2+(n+1/2)^2)\,\{E[a^2+(n+1/2)^2]\pi^2+\mathrm{Re}\,\rho\}} \\ &> \frac{\left|(a^2+(n+1+1/2)^2)\pi^2\mathrm{Im}\,\rho - a\pi\right|}{\pi^2(a^2+(n+1+1/2)^2)\,\{E[a^2+(n+1+1/2)^2]\pi^2+\mathrm{Re}\,\rho\}} \\ &= \left|\frac{\mathrm{Im}\,d_{n+1}}{\mathrm{Re}\,d_{n+1}}\right|.\end{aligned}$$

This, together with induction on n, implies that

$$\frac{|\mathrm{Im}\,\gamma_1|}{\mathrm{Re}\,\gamma_1} < \left|\frac{\mathrm{Im}\,d_1}{\mathrm{Re}\,d_1}\right|.$$

Thus we have

$$\left|\frac{\mathrm{Im}\,(-d_0-i)}{-\mathrm{Re}\,d_0}\right| < \left|\frac{\mathrm{Im}\,d_1}{\mathrm{Re}\,d_1}\right|,$$

and so

$$\frac{|2(a^2+1/4)\pi^2\mathrm{Im}\,\rho - 2a\pi - Ra(3/4-a^2)|}{(a^2+1/4)\mathrm{Re}\,\rho + E(a^2+1/4)^2\pi^2} < \frac{2|(a^2+9/4)\pi^2\mathrm{Im}\,\rho - a\pi|}{(a^2+9/4)\mathrm{Re}\,\rho + E(a^2+9/4)^2\pi^2}.$$

Therefore,

$$\begin{aligned}\frac{|2(a^2+1/4)\pi^2\mathrm{Im}\,\rho - 2a\pi - Ra(3/4-a^2)|}{2|(a^2+9/4)\pi^2\mathrm{Im}\,\rho - a\pi|} &< \frac{(a^2+1/4)[\mathrm{Re}\,\rho + E(a^2+1/4)\pi^2]}{(a^2+9/4)[\mathrm{Re}\,\rho + E(a^2+9/4)\pi^2]} \\ &\le \frac{a^2+1/4}{a^2+9/4},\end{aligned}$$

where we have used the condition $\mathrm{Re}\,\rho + E(a^2+1/4)\pi^2 > 0$. This implies

$$1 + \frac{Ra(3/4-a^2)}{2|(a^2+9/4)\pi^2\mathrm{Im}\,\rho - a\pi|} < \frac{a^2+1/4}{a^2+9/4} + \frac{2\pi^2|\mathrm{Im}\,\rho|}{|(a^2+9/4)\pi^2\mathrm{Im}\,\rho - a\pi|} < 1,$$

which leads to a contradiction and hence $\mathrm{Im}\,\rho > 0$. The proof of Lemma 3.2 is thus complete. ◻

LEMMA 3.3. *For one of the two eigenvalues obtained in Lemma* 3.1*, we have*

$$-\frac{1}{10} < \frac{2\pi^2}{a}\limsup_{R\to\infty}\frac{\mathrm{Im}\rho(R)}{R} < 2. \tag{3.5}$$

Proof. By (2.11), (2.12), and Lemma 2.2, we have

$$-\mathrm{Re}\,d_0|\xi_0|^2 > \mathrm{Re}\,d_1|\xi_1|^2,$$

or

$$-\mathrm{Re}\,d_0 > \mathrm{Re}\,d_1|d_0+i|^2.$$

Together with (2.7), this implies

$$\frac{(a^2+1/4)^2}{3/4-a^2} > \frac{(a^2+9/4)^2}{a^2+5/4}\left[\frac{2\pi^2(a^2+1/4)\mathrm{Im}\,\rho-2a\pi}{Ra(3/4-a^2)}-1\right]^2,$$

and so

$$\frac{(a^2+1/4)^2(a^2+5/4)}{(3/4-a^2)(a^2+9/4)^2} > \left[\frac{2\pi^2(a^2+1/4)}{a(3/4-a^2)}\limsup_{R\to\infty}\frac{\mathrm{Im}\,\rho}{R}-1\right]^2.$$

Therefore, the double inequality (3.5) holds for $\sqrt{3}/4 \le a < \sqrt{3}/2$ and the proof of Lemma 3.3 is thus complete. ∎

Now we prove the main result of this section.

THEOREM 3.4. *Let $\rho(R)$ be either one of the two complex conjugate eigenvalues obtained in Lemma* 3.1. *Then there exists a critical Reynolds number R_0 such that* $\mathrm{Re}\rho(R_0)=0$ *and* $\mathrm{Im}\rho(R_0)\neq 0$.

Proof. First, we prove the smoothness of $\rho(R)$ by using the implicit function theorem. Define the function

$$F(\rho,R) = i + d_0 + \cfrac{1}{d_1+\cfrac{1}{d_2+\cfrac{1}{\ddots}}} \tag{3.6}$$

with $d_n = d_n(\rho,R)$ given by (2.7). We see immediately that $F(\rho(R),R)=0$, due to (2.12) and Lemma 3.1. It follows from (3.4) that

$$\frac{\partial F(\rho,R)}{\partial\rho} = \sum_{n\ge 0}(-1)^n\frac{\partial d_n}{\partial\rho}\eta_n^2 = \sum_{n\neq 0}(-1)^n\frac{2\pi[a^2+(n+1/2)^2]}{Ra[(a^2+(n+1/2)^2-1]}\eta_n^2, \tag{3.7}$$

where $\{\eta_n\}$ is the solution specified by Lemma 2.2 such that $\eta_0=1$. Hence we have, by (2.11), that

$$\begin{aligned}
\left|\frac{\partial F(\rho,R)}{\partial\rho}\right| &\ge \frac{2\pi^2(a^2+1/4)}{Ra(3/4-a^2)}|\eta_0|^2 - \sum_{n\ge 1}\frac{2\pi^2[a^2+(n+1/2)^2]}{Ra[a^2+(n+1/2)^2-1]}|\eta_n|^2 \\
&= \frac{2\pi^2}{Ra}\sum_{n\ge 1}\frac{[a^2+(n+1/2)^2][\mathrm{Re}\rho+E\pi^2(a^2+(n+1/2)^2]}{[\mathrm{Re}\rho+E\pi^2(a^2+1/4)][a^2+(n+1/2)^2-1]}|\eta_n|^2 \\
&\quad -\sum_{n\ge 1}\frac{2\pi^2[a^2+(n+1/2)^2]}{Ra[a^2+(n+1/2)^2-1]}|\eta_n|^2 \\
&= \frac{2\pi^4 E}{\mathrm{Re}\rho+E\pi^2(a^2+1/4)}\sum_{n\ge 1}\frac{[a^2+(n+1/2)^2](n+1)n}{Ra[a^2+(n+1/2)^2-1]}|\eta_n|^2 > 0.
\end{aligned} \tag{3.8}$$

Thus, by the implicit function theorem, $\rho=\rho(R)$ is continuously differentiable.

Next, letting $R\to 0$ in (2.7) and (2.12), we see that

$$\lim_{R\to 0}\mathrm{Re}\,\rho(R) = -E\pi^2(a^2+1/4).$$

Finally, by Lemma 3.2 and the smoothness of $\rho(R)$, it suffices to show that

$$\limsup_{R\to\infty}\mathrm{Re}\,\rho(R) > 0.$$

To do so, we suppose that $\limsup_{R\to\infty} \operatorname{Re}\rho(R) \le 0$, which will lead to a contradiction.

Without loss of generality, by Lemma 3.3, we may suppose that

$$\lim_{R\to\infty} \operatorname{Re}\rho(R) = \mu, \quad \lim_{R\to\infty} \frac{2\pi^2 \operatorname{Im}\rho(R)}{Ra} = \nu \tag{3.9}$$

for some constants μ and ν. Otherwise, we may consider instead a subsequence $\{R_n\}$ that converges to these values.

Applying (2.12) and Lemma 2.2 yields

$$-d_0 - i = \frac{1}{d_1 + \frac{1}{d_2 + \gamma_3}}. \tag{3.10}$$

Hence

$$\begin{aligned} \lim_{R\to\infty} \gamma_3 &= \frac{1}{-\frac{1}{\lim_{R\to\infty} i\operatorname{Im} d_0 + i} - \lim_{R\to\infty} i\operatorname{Im} d_1} - \lim_{R\to\infty} i\operatorname{Im} d_2 \\ &= i\frac{\lim_{R\to\infty} \operatorname{Im} d_0 + 1}{\lim_{R\to\infty} \operatorname{Im} d_1 (\lim_{R\to\infty} \operatorname{Im} d_0 + 1) - 1} - \lim_{R\to\infty} i\operatorname{Im} d_2, \end{aligned} \tag{3.11}$$

or

$$\lim_{R\to\infty} (\operatorname{Im}\gamma_3 + \operatorname{Im} d_2) = \frac{\lim_{R\to\infty} \operatorname{Im} d_0 + 1}{\lim_{R\to\infty} \operatorname{Im} d_1(\operatorname{Im} d_0 + 1) - 1}. \tag{3.12}$$

Furthermore, it follows from (3.10) that

$$-d_0 - i = \frac{d_2 + \gamma_3}{d_1(d_2+\gamma_3) + 1} = \frac{(d_2+\gamma_3)(\overline{d_1(d_2+\gamma_3)} + 1)}{|d_1(d_2+\gamma_3)+1|^2},$$

and thus

$$\begin{aligned} &-\operatorname{Re} d_0 |d_1(d_2+\gamma_3)+1|^2 \\ &= \operatorname{Re}(d_2+\gamma_3)\operatorname{Re}(d_1(d_2+\gamma_3)+1) - \operatorname{Im}(d_2+\gamma_3)\operatorname{Im}\overline{d_1(d_2+\gamma_3)} \\ &= \operatorname{Re}(d_2+\gamma_3)(\operatorname{Re} d_1 \operatorname{Re}(d_2+\gamma_3) + 1) + \operatorname{Re} d_1 (\operatorname{Im} d_2 + \operatorname{Im}\gamma_3)^2. \end{aligned} \tag{3.13}$$

Multiplying the last equation by R and passing to the limit $R \to \infty$, we obtain, after using (3.9), (3.11), (3.12), and the positivity of $\operatorname{Re}\gamma_3$,

$$\begin{aligned} \lim_{R\to\infty} R|\operatorname{Re} d_0| &= \frac{\lim_{R\to\infty} R\operatorname{Re}(d_2+\gamma_3) + \lim_{R\to\infty} R\operatorname{Re} d_1 \lim_{R\to\infty} (\operatorname{Im} d_2 + \operatorname{Im}\gamma_3)^2}{|\lim_{R\to\infty} \operatorname{Im} d_1 \lim_{R\to\infty} (\operatorname{Im} d_2 + \operatorname{Im}\gamma_3) - 1|^2} \\ &\ge \frac{\lim_{R\to\infty} R\operatorname{Re} d_2 + \lim_{R\to\infty} R\operatorname{Re} d_1 \lim_{R\to\infty} (\operatorname{Im} d_2 + \operatorname{Im}\gamma_3)^2}{|\lim_{R\to\infty} \operatorname{Im} d_1 \lim_{R\to\infty} (\operatorname{Im} d_2 + \operatorname{Im}\gamma_3) - 1|^2} \\ &= \lim_{R\to\infty} R\operatorname{Re} d_1 (\lim_{R\to\infty} \operatorname{Im} d_0 + 1)^2 \\ &\quad + \lim_{R\to\infty} R\operatorname{Re} d_2 (1 - \lim_{R\to\infty} \operatorname{Im} d_1 (\operatorname{Im} d_0 + 1))^2. \end{aligned}$$

That is,

$$\begin{aligned}
&\frac{a^2+1/4}{3/4-a^2}\left[\mu+E(a^2+1/4)\pi^2\right]\\
&\geq \frac{a^2+9/4}{a^2+5/4}\left[\mu+E(a^2+9/4)\pi^2\right]\left(1-\frac{a^2+1/4}{3/4-a^2}\nu\right)^2\\
&\quad+\frac{a^2+25/4}{a^2+21/4}\left[\mu+E(a^2+25/4)\pi^2\right]\left[\frac{a^2+9/4}{a^2+5/4}\left(1-\frac{a^2+1/4}{3/4-a^2}\nu\right)\nu-1\right]^2.
\end{aligned}$$

This, together with the condition $-E(a^2+1/4)\pi^2 \leq \mu \leq 0$, implies

$$\begin{aligned}
\frac{(a^2+1/4)^2}{3/4-a^2} &\geq \frac{(a^2+9/4)^2}{a^2+5/4}\left(1-\frac{a^2+1/4}{3/4-a^2}\nu\right)^2\\
&\quad+\frac{(a^2+25/4)^2}{a^2+21/4}\left[1-\frac{a^2+9/4}{a^2+5/4}\left(1-\frac{a^2+1/4}{3/4-a^2}\nu\right)\nu\right]^2\\
&> \frac{(a^2+1/4)^2}{3/4-a^2}
\end{aligned}\tag{3.14}$$

for $\sqrt{3}/4 \leq a \leq \alpha_0$, with $\alpha_0 \simeq 0.80$. This leads to a contradiction and hence $\lim_{R\to\infty} \operatorname{Re}\rho > 0$. The proof of Theorem 3.4 is thus complete. ∎

4. Spectral simplicity condition. This section is devoted to the simplicity of each of the two complex conjugate eigenvalues that cross the imaginary axis. We prove the following theorem.

THEOREM 4.1. *Let the critical Reynolds number R_0 and the eigenvalue $\rho = \rho(R_0)$ with* $\operatorname{Im}\rho > 0$ *be as shown to exist in Theorem* 3.4. *Then this eigenvalue is simple, i.e.,*

$$\dim \bigcup_{n\geq 1} \left\{\phi \in H^4;\ L^n\phi = 0\right\} = 1, \tag{4.1}$$

where $L = L(\rho)$ is the linear operator defined in (1.5).

Proof. We introduce the invariant subspaces of the spectral problem (1.5) for any integer m:

$$E_{m,k} = \left\{\phi \in H^4;\ \psi(x,y) = \sum_{n\geq 1-k} i^n\phi_n e^{ima\pi x}\sin(n+k/2)\pi y\right\},\ \ k=0,1.$$

Hence the simplicity condition holds true provided that the following assertions are valid:

$$\dim \bigcup_{n\geq 1} \{\phi \in E_{m,k};\ L^n\phi = 0\} = 0 \tag{4.2}$$

for $(m,k) \neq (1,1)$, and

$$\dim \bigcup_{n\geq 1} \{\phi \in E_{1,1};\ L^n\phi = 0\} = 1. \tag{4.3}$$

Equation (4.2) follows immediately from Lemmas 2.1 and 2.2. Thus it remains to prove (4.3). We first note from Lemma 2.2 and Theorem 3.4 that

$$\dim\{\phi \in E_{1,1};\ L\phi = 0\} = 1.$$

By induction, it suffices to show

$$\dim\left\{\phi \in E_{1,1}\,;\ \ L^2\phi = 0\right\} = 1. \tag{4.4}$$

Indeed, rewrite the equation $L^2\phi = 0$ as

$$L\chi = 0, \tag{4.5}$$

after setting

$$L\phi = \chi \tag{4.6}$$

for some $\phi \in E_{1,1}$. It remains to show that $\phi \equiv 0$. Following the derivation of (2.10), we obtain the equivalent formulation of (4.5) and (4.6) in terms of two coupled difference equations:

$$\begin{cases} d_n\xi'_n - \xi'_{n-1} + \xi'_{n+1} = \xi_n, & n \geq 1, \\ d_n\xi_n - \xi_{n-1} + \xi_{n+1} = 0, & n \geq 1, \\ d_0\xi'_0 + i\xi'_0 + \xi'_1 = \xi_0, & n = 0, \\ d_0\xi_0 + i\xi_0 + \xi_1 = 0, & n = 0; \end{cases} \tag{4.7}$$

here d_n is defined by (2.7) and $\{\xi_n/d_n\}$, $\{\xi'_n\} \in l_2^2$, while l_2^2 denotes the Hilbert space

$$l_2^2 = \left\{ \{\xi_n\};\ \|\{\xi_n\}\|^2_{l_2^2} = \sum_{n\geq 0} n^2|\xi_n|^2 < \infty \right\}.$$

Define an operator $M : l_2^2 \mapsto l_2^2$ such that $M\{\xi_n\} = \{\eta_n\}$ with

$$\eta_n = \frac{1}{d_n}(\xi_{n+1} - \xi_{n-1}),\ \ \eta_0 = \frac{1}{d_0}(i\xi_0 + \xi_1),\ \ n \geq 1.$$

Equation (4.7) becomes

$$\begin{cases} (1+M)\{\xi'_n\} = \left\{\dfrac{\xi_n}{d_n}\right\}, \\ (1+M)\{\xi_n\} = 0. \end{cases} \tag{4.8}$$

We see that M is compact in l_2^2. It follows from Riesz–Schauder theory (also called the Fredholm alternative principle; see Theorem 5.3 in [15]) that (4.8) is solvable if and only if

$$\sum_{n\geq 0} \frac{\xi_n\bar{\zeta}_n}{d_n} = 0 \tag{4.9}$$

whenever $\{\zeta_n\} \in l_2^2$ is a nontrivial solution of the dual equation

$$(1+M^*)\{\zeta_n\} = 0, \tag{4.10}$$

where M^* is the dual operator of M.

Such a nontrivial solution of (4.10) is given by

$$\zeta_n + \frac{\zeta_{n-1}}{\bar{d}_{n-1}} - \frac{\zeta_{n+1}}{\bar{d}_{n+1}} = 0, \; n \geq 1,$$
$$\zeta_0 - \frac{i\zeta_0}{\bar{d}_0} - \frac{\zeta_1}{\bar{d}_1} = 0, \; n = 0.$$

This becomes, by setting $\hat{\zeta}_n = (-1)^n \bar{\zeta}_n / d_n$,

$$d_n \hat{\zeta}_n - \hat{\zeta}_{n-1} + \hat{\zeta}_{n+1} = 0, \; n \geq 1,$$
$$d_0 \hat{\zeta}_0 + i\hat{\zeta}_0 + \hat{\zeta}_1 = 0, \; n = 0.$$

By Lemma 2.2 and Theorem 3.4, we have

$$\hat{\zeta}_n = (-1)^n \frac{\bar{\zeta}_n}{d_n} = c\xi_n, \;\; n \geq 0,$$

for some constant $c \neq 0$. Thus (4.9) becomes

$$\sum_{n\geq 0} \frac{\xi_n \bar{\zeta}_n}{d_n} = c \sum_{n \geq 0} (-1)^n \xi_n^2 = 0.$$

Hence, it follows from (2.11) that

$$\begin{aligned} 0 &= \left| \sum_{n\geq 0} (-1)^n \xi_n^2 \right| \\ &\geq |\xi_0|^2 - \sum_{n\geq 1} |\xi_n|^2 \\ &= \frac{1}{|\mathrm{Re}\, d_0|} \sum_{n \geq 1} (\mathrm{Re}\, d_n - |\mathrm{Re}\, d_0|)|\xi_n|^2. \end{aligned}$$

Since $\mathrm{Re}\, d_n - |\mathrm{Re}\, d_0| > 0$ for $\sqrt{3}/4 \leq a < \sqrt{3}/2$, we thus have $\{\xi_n\} = 0$ and hence (4.4). The proof of Theorem 4.1 is complete. ∎

5. Transversal crossing condition. The objective of this section is to show that the pair of eigenvalues $\{\rho(R), \bar{\rho}(R)\}$) crosses the imaginary axis transversally and away from the origin. This result reads as follows.

THEOREM 5.1. *Let $\rho = \rho(R_0)$ and R_0 be as characterized in Lemma* 2.2 *and Theorems* 3.4 *and* 4.1. *Then the transversal crossing condition* (1.7) *holds, provided that $E > c_0$ for some constant $c_0 > 0$.*

Proof. Recalling the definition of the function $F = F(\rho, R)$ in (3.6), we see that the eigenvalue $\rho = \rho(R)$ satisfies the equation $F(\rho(R), R) = 0$, and so

$$\frac{\partial F}{\partial \rho} \frac{\mathrm{d}\rho(R)}{dR} + \frac{\partial F}{\partial R} = 0.$$

It follows from the derivation of (3.7) that

$$\frac{\partial F}{\partial R} = -\frac{1}{R} \sum_{n\geq 0} (-1)^n d_n \eta_n^2.$$

Thus, by (2.7) with $R = R_0$, (3.7), and (3.8), we have

$$\pi R_0 \mathrm{Re}\, \frac{\mathrm{d}\rho(R_0)}{\mathrm{d}R} = \pi \mathrm{Re}\, \frac{\displaystyle\sum_{n\geq 0} (-1)^n d_n \eta_n^2}{\displaystyle\sum_{n\geq 0} (-1)^n \frac{\partial d_n}{\partial \rho} \eta_n^2} = \mathrm{Re}\, \frac{\displaystyle\sum_{n\geq 0} (-1)^n \frac{\pi^3 E [a^2 + (n+1/2)^2]^2 - ia}{a^2 + (n+1/2)^2 - 1} \eta_n^2}{\displaystyle\sum_{n\geq 0} (-1)^n \frac{a^2 + (n+1/2)^2}{a^2 + (n+1/2)^2 - 1} \eta_n^2}.$$

This equals, after setting $a^2 + (n+1/2)^2 = \beta_n$,

$$\mathrm{Re}\, \frac{\displaystyle\sum_{n\geq 0} (-1)^n \frac{\pi^3 E \beta_n^2 - ia}{\beta_n - 1} \eta_n^2}{\displaystyle\sum_{n\geq 0} (-1)^n \frac{\beta_n}{\beta_n - 1} \eta_n^2}$$
$$= \pi^3 E \beta_0 + \sum_{n\geq 1} (-1)^n \frac{\pi^3 E \beta_n (\beta_n - \beta_0)}{\beta_n - 1} \mathrm{Re}\,(\xi_n^2) - \frac{a}{\beta_0} \sum_{n\geq 1} (-1)^n \frac{\beta_n - \beta_0}{\beta_n - 1} \mathrm{Im}\,(\xi_n^2),$$

where the solution $\{\xi_n\}$ is chosen such that

$$\xi_0^2 = \frac{1}{\displaystyle\sum_{n\geq 0} (-1)^n \frac{\beta_n}{\beta_n - 1} \eta_n^2}. \tag{5.1}$$

We thus have

$$\pi R_0 \mathrm{Re}\, \frac{\mathrm{d}\rho(R_0)}{\mathrm{d}R}$$
$$= \pi^3 E \beta_0 \left[1 - \frac{1}{\beta_0} \sum_{n\geq 1} \frac{\beta_n (\beta_n - \beta_0)}{\beta_n - 1} |\xi_n|^2 \right] - \frac{a}{\beta_0} \sum_{n\geq 1} (-1)^n \frac{\beta_n - \beta_0}{\beta_n - 1} \mathrm{Im}\,(\xi_n^2)$$
$$+ \pi^3 E \sum_{n\geq 1} \frac{\beta_n (\beta_n - \beta_0)}{\beta_n - 1} [|\xi_n|^2 + (-1)^n \mathrm{Re}\,(\xi_n^2)].$$

Furthermore, by (2.11) and (5.1), we have

$$1 - \frac{1}{\beta_0} \sum_{n\geq 1} \frac{\beta_n (\beta_n - \beta_0)}{\beta_n - 1} |\xi_n|^2$$
$$= 1 - \frac{1}{\beta_0} \sum_{n\geq 1} \frac{\beta_n^2}{\beta_n - 1} |\xi_n|^2 + \sum_{n\geq 1} \frac{\beta_n}{\beta_n - 1} |\xi_n|^2$$

$$
\begin{aligned}
&= |\xi_0|^2 \left[\left| \sum_{n\geq 0} (-1)^n \frac{\beta_n}{\beta_n - 1} \eta_n^2 \right| + \sum_{n\geq 1} \frac{\beta_n}{\beta_n - 1} |\eta_n|^2 + \frac{\beta_0}{\beta_0 - 1} \right] \\
&\geq |\xi_0|^2 \left[\left| \sum_{n\geq 0} (-1)^n \frac{\beta_n}{\beta_n - 1} \mathrm{Re}\,(\eta_n^2) \right| + \sum_{n\geq 1} \frac{\beta_n}{\beta_n - 1} |\eta_n|^2 + \frac{\beta_0}{\beta_0 - 1} \right] \\
&\geq |\xi_0|^2 \sum_{n\geq 1} \frac{\beta_n}{\beta_n - 1} |\eta_n|^2 - |\xi_0|^2 \left| \sum_{n\geq 1} (-1)^n \frac{\beta_n}{\beta_n - 1} \mathrm{Re}\,(\eta_n^2) \right| \\
&\geq |\xi_0|^2 \frac{\beta_1}{\beta_1 - 1} (|\eta_1|^2 - |\mathrm{Re}\,(\eta_1^2)|),
\end{aligned}
$$

and

$$
\begin{aligned}
\left| \sum_{n\geq 1} (-1)^n \frac{\beta_n - \beta_0}{\beta_n - 1} \mathrm{Im}\,(\xi_n^2) \right| &\leq \sum_{n\geq 1} \frac{\beta_n - \beta_0}{\beta_n - 1} |\mathrm{Im}\,(\xi_n^2)| \\
&\leq \frac{1}{\beta_1} \sum_{n\geq 1} \frac{\beta_n^2}{\beta_n - 1} |\xi_n|^2 = \frac{\beta_0^2}{\beta_1(1-\beta_0)} |\xi_0|^2.
\end{aligned}
$$

Collecting terms while using (2.12) and Lemma 2.2, we have

$$
\begin{aligned}
&\frac{R_0}{\pi^2 |\xi_0|^2} \mathrm{Re}\, \frac{\mathrm{d}\rho(R_0)}{\mathrm{d}R} \\
&\geq E\beta_0(|\eta_1|^2 - |\mathrm{Re}\,\eta_1^2|) + E(\beta_1 - \beta_0) \left(|\eta_1|^2 - \frac{\mathrm{Re}\,\xi_1^2}{|\xi_0|^2} \right) - \frac{a\beta_0}{\pi^3 \beta_1 (1-\beta_0)} \\
&= E\beta_0(|d_0 + i|^2 - |\mathrm{Re}\,(d_0 + i)^2|) \\
&\quad + 2E \left(|d + i|^2 - \frac{\mathrm{Re}\,[(d_0 + i)^2 \xi_0^2]}{|\xi_0|^2} \right) - \frac{a\beta_0}{\pi^3 \beta_1 (1-\beta_0)}.
\end{aligned}
$$

Let us now apply the following lemma, whose proof will be given at the end of this section.

LEMMA 5.2. *One of the following two estimates,*

$$
\liminf_{E\to\infty} \frac{E}{R_0} > 0 \tag{5.2}
$$

or

$$
\liminf_{E\to\infty} |\mathrm{Re}\; d_0| > 0, \tag{5.3}
$$

holds true.

If $|1 + \mathrm{Im}\, d_0| > |\mathrm{Re}\, d_0|$, we have

$$
\begin{aligned}
\frac{R_0}{\pi^2 |\xi_0|^2} \mathrm{Re}\, \frac{\mathrm{d}\rho(R_0)}{\mathrm{d}R} &\geq E\beta_0(|d_0 + i|^2 - |\mathrm{Re}\,(d_0 + i)^2|) - \frac{a\beta_0}{\pi^3 \beta_1 (1-\beta_0)} \\
&= 2E\beta_0 (\mathrm{Re}\, d_0)^2 - \frac{a\beta_0}{\pi^3 \beta_1 (1-\beta_0)};
\end{aligned}
$$

the latter is positive due to Lemma 5.1, after letting $E > c_0$ for some constant $c_0 > 0$.

If $|\mathrm{Re}\, d_0| \geq |1 + \mathrm{Im}\, d_0| > |\mathrm{Re}\, d_0|/4$, we see that

$$\begin{aligned}\frac{R_0}{\pi^2|\xi_0|^2}\mathrm{Re}\,\frac{\mathrm{d}\rho(R_0)}{\mathrm{d}R} &\geq E\beta_0(|d_0+i|^2 - |\mathrm{Re}\,(d_0+i)^2|) - \frac{a\beta_0}{\pi^3\beta_1(1-\beta_0)} \\ &= 2E\beta_0(1+\mathrm{Im}\, d_0)^2 - \frac{a\beta_0}{\pi^3\beta_1(1-\beta_0)} \\ &\geq \frac{1}{2}E\beta_0(\mathrm{Re}\, d_0)^2 - \frac{a\beta_0}{\pi^3\beta_1(1-\beta_0)} > 0,\end{aligned}$$

which is positive as well for E large enough.

For the remaining case $|\mathrm{Re}\, d_0|/4 \geq |1+\mathrm{Im}\, d_0| \geq 0$, we see that $-\mathrm{Re}\,(\xi_0^2) > 0$ due to (2.11) and (5.1). Hence we have

$$\begin{aligned}&\frac{R_0}{\pi^2|\xi_0|^2}\mathrm{Re}\,\frac{\mathrm{d}\rho(R_0)}{\mathrm{d}R} \\ &\geq 2E\left\{|d+i|^2 - \frac{\mathrm{Re}\,[(d_0+i)^2\xi_0^2]}{|\xi_0|^2}\right\} - \frac{a\beta_0}{\pi^3\beta_1(1-\beta_0)} \\ &\geq 2E\left[|d+i|^2 + \frac{2(\mathrm{Re}\, d_0)(1+\mathrm{Im}\, d_0)\mathrm{Im}\,(\xi_0^2)}{|\xi_0|^2}\right] - \frac{a\beta_0}{\pi^3\beta_1(1-\beta_0)} \\ &\geq E(\mathrm{Re}\, d_0)^2 - \frac{a\beta_0}{\pi^3\beta_1(1-\beta_0)}.\end{aligned}$$

This also implies the desired assertion by letting E be large enough. The proof of Theorem 5.1 is complete, subject to proving Lemma 5.2. ∎

Proof of Lemma 5.2. Let us first note, from (2.11) and Lemma 2.2, that

$$\mathrm{Re}\, d_1|\eta_1|^2 < -\mathrm{Re}\, d_0,$$

or, by (2.12),

$$\frac{\beta_0^2(\beta_1-1)}{\beta_1^2(1-\beta_0)} > |d_0+i|^2 = \left[\frac{2\pi^2\beta_0\mathrm{Im}\,\rho - a\pi}{R_0a(1-\beta_0)} - 1\right]^2 + \left[\frac{2\pi^4E\beta_0^2}{R_0a(1-\beta_0)}\right]^2. \tag{5.4}$$

This implies

$$|d_1| + |d_2| < c_1, \tag{5.5}$$

and $R_0 > c_2E$ for some positive constants c_1 and c_2, independent of E and R_0. Thus $E \to \infty$ implies $R_0 \to \infty$.

On the contrary, we suppose that

$$\liminf_{E\to\infty} \frac{E}{R_0} = 0, \tag{5.6}$$

which will lead to a contradiction. Indeed, by following the final step in the proof of Theorem 3.1, we use (2.12) or (3.10) to obtain

$$\begin{aligned}\lim_{E\to\infty}\gamma_3 &= \frac{1}{-\dfrac{1}{\lim\limits_{E\to\infty} i\mathrm{Im}\, d_0 + i} - \lim\limits_{E\to\infty} i\mathrm{Im}\, d_1} - \lim_{E\to\infty} i\mathrm{Im}\, d_2 \\ &= i\frac{\lim\limits_{E\to\infty}\mathrm{Im}\, d_0 + 1}{\lim\limits_{E\to\infty}\mathrm{Im}\, d_1(\lim\limits_{E\to\infty}\mathrm{Im}\, d_0 + 1) - 1} - \lim_{E\to\infty} i\mathrm{Im}\, d_2\end{aligned} \tag{5.7}$$

and

$$\lim_{E\to\infty}(\operatorname{Im}\gamma_3+\operatorname{Im}d_2)=\frac{\lim_{E\to\infty}\operatorname{Im}d_0+1}{\lim_{E\to\infty}\operatorname{Im}d_1(\operatorname{Im}d_0+1)-1}, \tag{5.8}$$

where, for simplicity of notation, we have supposed the existence of the limit.

Furthermore, multiplying (3.13) by R_0/E and passing to the limit $E\to\infty$, we obtain, after applying (5.4), (5.5), (5.6), (5.7), (5.8), and the positivity of $\operatorname{Re}\gamma_3$,

$$\begin{aligned}\frac{R_0}{E}|\operatorname{Re}d_0| &= \frac{\lim_{E\to\infty}\frac{R_0}{E}\operatorname{Re}(d_2+\gamma_3)+\frac{R_0}{E}\operatorname{Re}d_1\lim_{E\to\infty}(\operatorname{Im}d_2+\operatorname{Im}\gamma_3)^2}{|\lim_{E\to\infty}\operatorname{Im}d_1\lim_{E\to\infty}(\operatorname{Im}d_2+\operatorname{Im}\gamma_3)-1|^2}\\ &\geq \frac{\frac{R_0}{E}\operatorname{Re}d_2+\frac{R_0}{E}\operatorname{Re}d_1\lim_{E\to\infty}(\operatorname{Im}d_2+\operatorname{Im}\gamma_3)^2}{|\lim_{E\to\infty}\operatorname{Im}d_1\lim_{E\to\infty}(\operatorname{Im}d_2+\operatorname{Im}\gamma_3)-1|^2};\end{aligned}$$

that is,

$$\begin{aligned}\frac{\beta_0^2}{1-\beta_0} &\geq \frac{\frac{\beta_2^2}{\beta_2-1}+\frac{\beta_1^2}{\beta_1-1}\lim_{E\to\infty}(\operatorname{Im}d_2+\operatorname{Im}\gamma_3)^2}{|\lim_{E\to\infty}\operatorname{Im}d_1\lim_{E\to\infty}(\operatorname{Im}d_2+\operatorname{Im}\gamma_3)-1|^2}\\ &\geq \frac{\beta_2^2}{\beta_2-1}[1-\lim_{E\to\infty}\operatorname{Im}d_1(\operatorname{Im}d_0+1)]^2\\ &\geq \frac{\beta_2^2}{\beta_2-1}\left[1-\frac{\beta_1(1-\beta_0)}{4\beta_0(\beta_1-1)}\right]^2.\end{aligned}$$

We thus have

$$\frac{(a^2+1/4)^2}{3/4-a^2}\geq\frac{(a^2+25/4)^2}{a^2+21/4}\left[1-\frac{(a^2+9/4)(3/4-a^2)}{4(a^2+1/4)(a^2+5/4)}\right]^2>\frac{(a^2+1/4)^2}{3/4-a^2}.$$

This leads to a contradiction for $\sqrt{3}/4\leq a\leq\alpha_0$, and hence (5.2) is valid. The proof of Lemma 5.2, and hence that of Theorem 5.1, is complete. □

As stated in section 1, assertion (i) of Theorem 1.1 was proven in section 2, while assertion (ii) follows by combining the results of Theorems 3.4, 4.1, and 5.1.

6. Numerical experiments. In this section, we compute numerically the Hopf bifurcation of the zonally periodic problem (1.1) with boundary conditions given by (1.2) and for various values of the aspect ratio a. We discretize a steady-state version of (1.1), as well as the spectral problem (1.5), both using the free-slip boundary conditions (1.2). The finite-difference discretization uses the Arakawa scheme, which conserves energy and enstrophy for 2-D incompressible flows [1]. The spatial resolution is $\Delta x=\Delta y=0.0249$; i.e., there are $N=80$ points in the y direction, $N\Delta y=2$; this resolution is kept the same for all values of a tested ($0.2\leq a\leq 0.86$).

The basic solution $\psi_0=\psi_0(x_i,y_i)$ is found by a pseudoarclength continuation algorithm [9, 23, 39, 42] that solves the discretized steady-state version of (1.1) instead of using (1.3). In order to solve the spectral problem (1.5) we compute the first 10 leading eigenvalues of its discretized version, i.e., those that are closest to the imaginary axis, since it is prohibitive to compute the whole spectrum for our resolution

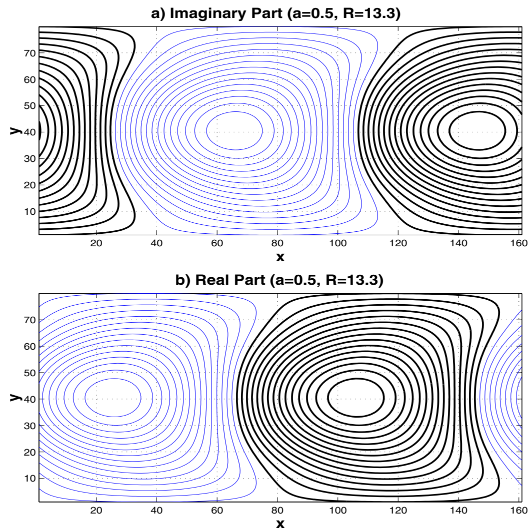

FIG. 6.1. *Unstable oscillatory mode for $a = 0.5$ and $R = 13.3$:* (a) *Imaginary part ($t = -T/4$); and* (b) *real part ($t = 0$). Light contour lines correspond to negative values and heavy contours to positive ones.*

of $N \times N/a = O(10^4)$ variables. This is achieved using a spectral transformation of the problem combined with a simultaneous iteration technique algorithm (see [39, 40, 42]). An oscillatory eigenfunction $\boldsymbol{\Phi_r} + i\boldsymbol{\Phi_i}$ and the corresponding pair of complex conjugate eigenvalues $\kappa_r \pm i\kappa_i$ provide the time-periodic disturbance structure $\boldsymbol{\Phi}(t)$ with angular frequency κ_i and growth rate κ_r, i.e.,

$$\boldsymbol{\Phi}(t) = \mathrm{e}^{\kappa_r t} \left[\boldsymbol{\Phi_r} \cos \kappa_i t - \boldsymbol{\Phi_i} \sin \kappa_i t\right]. \tag{6.1}$$

Figure 6.1 shows the spatial patterns of the leading eigenvector that loses its stability as R is increased. According to (6.1) this instability propagates westward and it does so for all aspect ratios a we used. The dipolar east-west structure of the destabilizing perturbation is also independent of a. The time-periodic solution is thus characterized by a westward propagation of alternating positive and negative vortices. When a nonlinearly saturated, finite-amplitude version of this oscillatory mode is added to the basic zonal flow Ψ_0, it results in a meandering of the eastward jet (not shown).

The numerically obtained spatial patterns also confirm the theoretical result that this instability is symmetric with respect to the midaxis of the channel. Moreover, numerical results tend to show that there is no other 2-D instability but this one: for fairly large values of $R >> R_0$, there is no other eigenvalue that crosses the imaginary axis.

We now investigate the value of the critical Reynolds number R_0 at the Hopf bifurcation, as a function of the aspect ratio a. We also compute the period $T = 2\pi/\kappa_i$ of the instability at R_0. Both the curves $R_0 = R_0(a)$ and $T = T(a)$ are shown in Figures 6.2(a) and 6.2(b), respectively. The vertical asymptote in both panels strongly suggests that for $a \geq \sqrt{3}/2$ the flow is linearly stable around Ψ_0, in excellent agreement with Theorem 1.1.

Both curves are continuous and monotonic across the entire interval $\sqrt{3}/4 \leq a < \sqrt{3}/2$. This indicates that the difficulties in proving Hopf bifurcation for $\alpha_0 \leq a <$

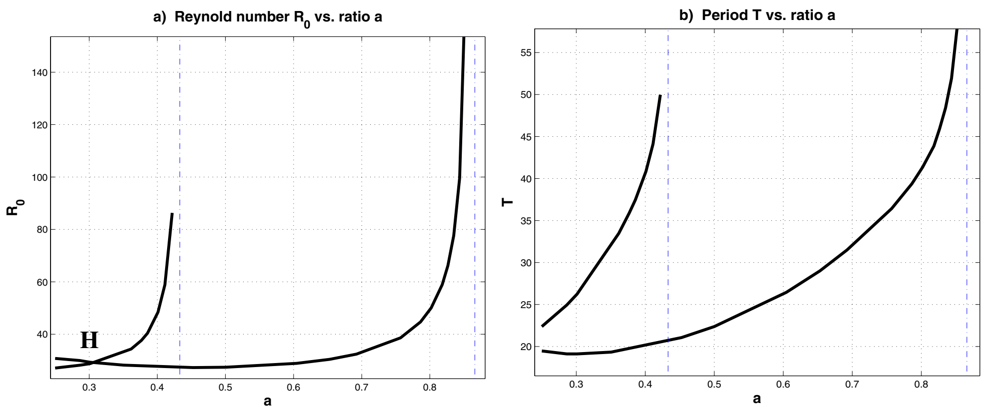

FIG. 6.2. *Dependence of the model's oscillatory instabilities on the aspect ratio a:* (a) *Critical Reynolds number R_0; and* (b) *period T of the limit cycle at Hopf bifurcation. T has been nondimensionalized by L/U with $L = 4000$ km and $U = 15$ ms^{-1}. The vertical dash-dotted straight lines correspond to $a = \sqrt{3}/4$ and $a = \sqrt{3}/2$, respectively. H refers to the simultaneous crossing of the imaginary axis by two distinct eigenmodes, with wavenumbers $m = 1$ and $m = 2$, respectively.*

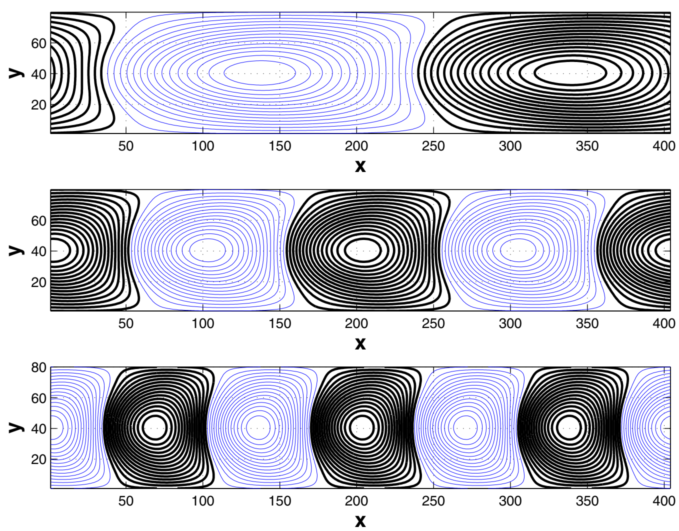

FIG. 6.3. *Real parts of the three unstable modes for $a = 0.2$ and $R = 26.6$.*

$\sqrt{3}/2$ are purely technical. In this interval, the flow becomes unstable as well, with a spatial pattern that resembles Figure 6.1 (not shown). The period of the instability increases as the zonal length of the channel decreases and it tends to infinity as a tends to the critical value $\sqrt{3}/2$. Numerical experiments also confirm that only a single instability with wavenumber one is found in the interval $\sqrt{3}/4 \leq a < \sqrt{3}/2$.

For $a < \sqrt{3}/4$, interesting phenomena occur that are not captured by our Theorem 1.1. Numerical experiments indicate the existence of additional oscillatory instabilities, characterized by higher spatial harmonics, as shown in Figures 6.2 and 6.3. The competition between these instabilities is expected to generate chaotic dynamics as a is decreased. Codimension-2 Hopf–Hopf bifurcations, with complex global dynamics nearby, are likely to play a key role in this process. The first of these bifurcations is denoted in Figure 6.2(a) by H and it occurs at $a \simeq 0.31$. At $a = 0.2$ and $R = 26.6$ (not shown in Figure 6.2), three unstable modes, with $m = 1, 2, 3$, coexist. These modes are shown in Figure 6.3 and are all symmetric about the channel's midaxis.

To gain some geophysical insight into the nature of the fundamental instability, we select characteristic dimensional magnitudes for the width $2L$ of the channel and the maximum $\tau_0 U/\pi^3 E$ of the zonal velocity in the midlatitude atmospheric jet. The value of $L = 4000$ km thus yields a meridional extent of the channel of 8000 km. The choice of $U = 15$ ms^{-1} and E between 50 and 100 corresponds to maximum zonal jet velocities between 25 and 50 ms^{-1} that agree well with those observed. Taking the midaxis of the β-channel at 45° N, as is often done in theoretical studies of large-scale atmospheric flow, and $a \simeq 0.26$ yields a channel length of $2L/a$ that corresponds to about 360° in longitude.

With these choices of L, U, and a, the numerical results shown in Figures 6.2(b) and 6.3 yield periods of 20–25 days for the instabilities obtained. Of these, the second one, with zonal wavenumber $m = 2$, has about the correct dimensional wavelength to match the westward-traveling Branstator–Kushnir [3, 22] wave. This wave has been shown to have, indeed, an equivalent-barotropic, i.e., essentially 2-D, structure and a period of about 25 days [11, 12, 13].

7. Symmetry considerations. As discussed in section 1, the symmetry properties of the domain and the forcing, on the one hand, and of the perturbation that gives rise to the bifurcation, on the other, have a decisive effect on whether the bifurcation leads to a branch of stationary or oscillatory solutions. Legras and Ghil [23] and Jin and Ghil [19] pointed out that, in the atmospheric channel problem with bottom topography, back-to-back saddle-node bifurcations resulted when the zonal forcing jet had a flat or unimodal velocity profile; see also Charney and DeVore [6] and Pedlosky [35]. To the contrary, when a higher-order component, which exhibited an inflection point, was present in the forcing jet, an oscillatory instability with so-called intraseasonal periods of 30–60 days could set in by resonance with this higher-order component and lead to a stable limit cycle.

Traveling Rossby waves are the unique type of solutions of (1.1) in the same periodic-channel geometry and in the absence of forcing, topography, and dissipation. The longest known period of this type of so-called free Rossby wave is about 16 days (Madden [29]). The periods of the oscillatory instabilities obtained previously, with bottom topography [6, 19, 23, 35], and here without it, are considerably longer: 25–50 days. Our rigorous result in Theorem 1.1 shows that Hopf bifurcation occurs even for a flat bottom of the channel, in agreement with the numerical results of section 6. The separate effects of forcing and dissipation, on the one hand, and topography, on the other, on the period of oscillatory solutions will be studied further elsewhere.

In the oceanic rectangular-basin problem, on the other hand, given the antisymmetric wind-stress forcing profile of (1.1) here, a steady double-gyre circulation resulted that is antisymmetric with respect to the basin's zonal symmetry axis [4, 18, 42]. This circulation is first destabilized by a pitchfork bifurcation—perfect in QG models [4, 5, 14] and perturbed in shallow-water models [18, 40, 41]—that arises from a purely exponential instability, which is symmetric with respect to the symmetry axis defined here as $y = 1$. Oscillatory instabilities documented numerically in either type of model, QG or shallow-water, also included some that have an asymmetric spatial pattern. The periods of these asymmetric instabilities are also much longer than those of the oceanic problem's free modes (i.e., the Rossby basin modes arising in the absence of forcing and dissipation); see Simonnet and Dijkstra [39] and Simonnet et al. [41].

The symmetry properties of the Hopf bifurcation here are thus in agreement with those obtained numerically for the atmospheric channel flow. The situation for the oceanic double-gyre problem is more complex and requires further investigation. It might be possible, using some of these symmetry ideas, to adapt the approach and methods used here to this oceanic problem, in spite of the fact that analytic stationary solutions are harder to find for it [18, 44].

Acknowledgments. The first draft of this paper was prepared for presentation at the mathematical congress honoring the memory of Jacques-Louis Lions held in July 2002 at the Collège de France, Paris. It is a pleasure to thank the organizers and the participants of this congress for the impetus to complete the paper in its present form. Constructive comments by Gershon Wolansky and an anonymous reviewer helped improve the presentation and stimulated us to add section 6.

REFERENCES

[1] A. Arakawa, *Computational design for long-term numerical integrations of the equations of atmospheric motion*, J. Comput. Phys., 1 (1966), pp. 119–143.
[2] P. S. Berloff and S. P. Meacham, *On the stability of the wind-driven circulation*, J. Marine Res., 56 (1998), pp. 937–993.
[3] G. W. Branstator, *A striking example of the atmosphere's leading traveling pattern*, J. Atmospheric Sci., 44 (1987), pp. 2310–2323.
[4] P. Cessi and G. R. Ierley, *Symmetry-breaking multiple equilibria in quasi-geostrophic, wind-driven flows*, J. Phys. Oceanogr., 25 (1995), pp. 1196–1202.
[5] K.-I. Chang, M. Ghil, K. Ide, and C.-C. A. Lai, *Transition to aperiodic variability in a wind-driven double-gyre circulation model*, J. Phys. Oceanogr., 31 (2001), pp. 1260–1286.
[6] J. Charney and J. DeVore, *Multiple flow equilibria in the atmosphere and blocking*, J. Atmospheric Sci., 36 (1979), pp. 1205–1216.
[7] Z. M. Chen and W. G. Price, *Remarks on time-dependent periodic Navier-Stokes flow in a two-dimensional torus*, Comm. Math. Phys., 207 (1999), pp. 81–106.
[8] Z. M. Chen and S. Wang, *Steady-state bifurcations of the three-dimensional Kolmogorov problem*, Electron. J. Differential Equations, 58 (2000), pp. 1–32.
[9] H. A. Dijkstra, *Nonlinear Physical Oceanography: A Dynamical Systems Approach to the Large-Scale Ocean Circulation and El Niño*, Kluwer Acad. Publishers, Dordrecht, Norwell, MA, 2000.
[10] M. Ghil and S. Childress, *Topics in Geophysical Fluid Dynamics: Atmospheric Dynamics, Dynamo Theory, and Climate Dynamics*, Springer-Verlag, New York, 1987.
[11] M. Ghil and K.-C. Mo, *Intraseasonal oscillations in the global atmosphere. Part* I: *Northern Hemisphere and tropics*, J. Atmospheric Sci., 48 (1991), pp. 752–779.
[12] M. Ghil and K.-C. Mo, *Intraseasonal oscillations in the global atmosphere. Part* II: *Southern Hemisphere*, J. Atmospheric Sci., 48 (1991), pp. 780–790.
[13] M. Ghil and A. W. Robertson, *"Waves" vs. "particles" in the atmosphere's phase space: A pathway ro long-range forecasting?*, Proc. Natl. Acad. Sci., 99 (2002), pp. 2493–2500.
[14] M. Ghil, Y. Feliks, and L. Sushama, *Baroclinic and barotropic aspects of the wind-driven ocean circulation*, Phys. D, 167 (2002), pp. 1–35.
[15] D. Gilbarg and N. S. Trudinger, *Elliptic Partial Differential Equations of Second Order*, 2nd ed., Springer-Verlag, New York, 1983.
[16] G. Ierley and V. A. Sheremet, *Multiple solutions and advection-dominated flows in the wind-driven circulation* I: *Slip*, J. Marine Res., 53 (1995), pp. 703–737.
[17] V. I. Iudovich, *Example of the generation of a secondary stationary or periodic flow when there is loss of stability of the laminar flow of a viscous incompressible fluid*, J. Math. Mech., 29 (1965), pp. 587–603.
[18] S. Jiang, F.-F. Jin, and M. Ghil, *Multiple equilibria, periodic, and aperiodic solutions in a wind-driven, double-gyre, shallow-water model*, J. Phys. Oceanogr., 25 (1995), pp. 764–786.
[19] F.-F. Jin and M. Ghil, *Intraseasonal oscillations in the extratropics: Hopf bifurcation and topographic instabilities*, J. Atmospheric Sci., 47 (1990), pp. 3007–3022.

[20] D. D. Joseph and D. Sattinger, *Bifurcating time periodic solutions and their stability*, Arch. Ration. Mech. Anal., 45 (1972), pp. 75–109.
[21] E. Kalnay, *Atmospheric Modeling, Data Assimilation and Predictability*, Cambridge University Press, Cambridge, UK, in press.
[22] Y. Kushnir, *Retrograding wintertime low-frequency disturbances over the North Pacific Ocean*, J. Atmospheric Sci., 44 (1987), pp. 2727–2742.
[23] B. Legras and M. Ghil, *Persistent anomalies, blocking and variations in atmospheric predictability*, J. Atmospheric Sci., 42 (1985), pp. 433–471.
[24] J. L. Lions, R. Temam, and S. Wang, *New formulations of the primitive equations of atmosphere and applications*, Nonlinearity, 5 (1992), pp. 237–288.
[25] J. L. Lions, R. Temam, and S. Wang, *On the equations of large-scale ocean*, Nonlinearity, 5 (1992), pp. 1007–1053.
[26] E. N. Lorenz, *Deterministic nonperiodic flow*, J. Atmospheric Sci., 20 (1963), pp. 130–141.
[27] E. N. Lorenz, *The mechanics of vacillation*, J. Atmospheric Sci., 20 (1963), pp. 448–464.
[28] E. N. Lorenz, *The Nature and Theory of the General Circulation of the Atmosphere*, World Meteorological Organization, Geneva, Switzerland, 1967.
[29] R. A. Madden, *Observations of large-scale traveling Rossby waves*, Revs. Geophys., 17 (1979), pp. 1935–1949.
[30] J. E. Marsden and M. McCracken, *The Hopf Bifurcation and Its Applications*, Springer-Verlag, New York, 1976.
[31] S. P. Meacham, *Low-frequency variability in the wind-driven circulation*, J. Phys. Oceanogr., 30 (2000), pp. 269–293.
[32] S. P. Meacham and P. S. Berloff, *Instability of a steady, barotropic, wind-driven circulation*, J. Marine Res., 55 (1997), pp. 885–913.
[33] L. D. Meshalkin and Ya. G. Sinai, *Investigation of the stability of a stationary solution of a system of equations for the plane movement of an incompressible viscous fluid*, J. Math. Mech., 19 (1961), pp. 1700–1705.
[34] B. Nadiga and B. Luce, *Global bifurcation of Shilnikov type in a double gyre ocean model*, J. Phys. Oceanogr., 31 (2001), pp. 2669–2690.
[35] J. Pedlosky, *Resonant topographic waves in barotropic and baroclinic flows*, J. Atmospheric Sci., 38 (1981), pp. 2626–2641.
[36] J. Pedlosky, *Geophysical Fluid Dynamics*, 2nd ed., Springer-Verlag, New York, 1987.
[37] J. Shen, T. Tachim-Medjo, and S. Wang, *On a wind-driven, double-gyre, quasi-geostrophic ocean model: Numerical simulations and structural analysis*, J. Comp. Phys., 155 (1999), pp. 387–409.
[38] V. A. Sheremet, G. Ierley, and V. Kamenkovich, *Eigenanalysis of the two-dimensional wind-driven ocean circulation problem*, J. Marine Res., 55 (1997), pp. 57–92.
[39] E. Simonnet and H. Dijkstra, *Spontaneous generation of low-frequency modes of variability in the wind-driven ocean circulation*, J. Phys. Oceanogr., 32 (2002), pp. 1747–1762.
[40] E. Simonnet, M. Ghil, K. Ide, R. Temam, and S. Wang, *Low-frequency variability in shallow-water models of the wind-driven ocean circulation. Part* I: *Steady-state solutions*, J. Phys. Oceanogr., to appear.
[41] E. Simonnet, M. Ghil, K. Ide, R. Temam, and S. Wang, *Low-frequency variability in shallow-water models of the wind-driven ocean circulation. Part* II: *Time-dependent solutions*, J. Phys. Oceanogr., to appear.
[42] S. Speich, H. Dijkstra, and M. Ghil, *Successive bifurcations in a shallow-water model, applied to the wind-driven ocean circulation*, Nonlin. Proc. Geophys., 2 (1995), pp. 241–268.
[43] H. Stommel, *Thermohaline convection with two stable regimes of flow*, Tellus, 13 (1961), pp. 224–230.
[44] G. Veronis, *An analysis of wind-driven ocean circulation with a limited number of Fourier components*, J. Atmospheric Sci., 20 (1963), pp. 577–593.
[45] G. Veronis, *Wind-driven ocean circulation. Part* II: *Numerical solution of the nonlinear problem*, Deep-Sea Res., 13 (1966), pp. 30–55.
[46] S. Wang, *Attractors for the 3D baroclinic quasi-geostrophic equations of large-scale atmosphere*, J. Math. Anal. Appl., 165 (1992), pp. 266–283.
[47] G. Wolansky, *Existence, uniqueness, and stability of stationary barotropic flow with forcing and dissipation*, Comm. Pure Appl. Math., 41 (1988), pp. 19–46.
[48] G. Wolansky, *The barotropic vorticity equation under forcing and dissipation: Bifurcations of nonsymmetric responses and multiplicity of solutions*, SIAM J. Appl. Math., 49 (1989), pp. 1585–1607.